Robust Method for Camera Self-Calibration by an Unkown Planar Scene

A. Baataoui[1], N. El Akkad[1], A. Saaidi[1,2], K. Satori[1], Med. Masrar[1]

[1]LIIAN, Department of Mathematics and Computer Science, Faculty of Sciences,
Dhar El Mehraz, Sidi Mohamed Ben Abdellah University, B.P 1796, Atlas, Fez, Morocco.
[2]LIMAO, Department of Mathematics, Physics and Computer Science,
Polydisciplinary Faculty of Taza, Sidi Mohamed Ben Abdellah University, B.P 1223, Taza, Morocco.
baataoui.aziz@gmail.com, nabil_abdo80@yahoo.fr, saaidi.abde@yahoo.fr,
khalidsatorim3i@yahoo.fr, masrar.m@hotmail.com.

Abstract. In this paper, we present a method of self-calibration of a CCD camera with varying intrinsic parameters by an unknown planar scene. The advantage of our method is to reduce the number of images (two images) to estimate the parameters of the camera used. Moreover, the self-calibration equations become related to the number of matched points (very numerous and easy to detect) and not to the number of images, because the use of a large number of the images requires a high execution time. On the other hand, we base on the matched points which are numerous to estimate the projection matrices and the homographies between images. The latter are used with the images of the absolute conic to formulate a system of non-linear equations (self-calibration equations depend on the number of matched couples). Finally, the intrinsic parameters of the camera can be obtained by minimizing a non-linear cost function proceeding from two steps: initialization and optimization. The experiment results show the robustness of our algorithms in terms of stability and convergence.

Keywords: self-calibration, equilateral triangle, absolute conic, homography, varying intrinsic parameters.

1. Introduction

The camera is the main element in many applications of computer vision. The estimation of camera parameters is an important step in this kind of applications. Generally, the estimation procedure can be performed according to two strategies. The first is called the calibration: it consists to determine the intrinsic and extrinsic parameters using a known object (calibration pattern) [12, 14, 15, 25]. The latter can be three-dimensional (3D calibration) or plane (2D calibration). The second strategy is called self-calibration. It allows determining the intrinsic and extrinsic parameters without any prior knowledge of the scene. Several works are based on the self-calibration of cameras from 3D scenes [4–8, 13, 24, 31], or they are based on planar scenes [11, 18, 26, 28] to automatically determine the intrinsic and extrinsic parameters.

In this work, we are interested on the self-calibration of a camera with varying intrinsic parameters by any planar scene. We mention that from two points of the 2D scene

we can obtain an equilateral triangle (the third point of the triangle can be obtained in a unique way). Our method is based on the rotation of a fixed reference associated with the planar scene to determine the transformation matrix between the vertices of the different equilateral triangles. This transformation characterizes the strong point of our approach. The latter resides in the use of a large number of matches which are the projections of the points (two vertices of the equilateral triangles) of the planar scene in the couples of images. This projection is used with the homography matrices to formulate a system of linear equations. The resolution of the latter allows obtaining the projection matrices. After detecting the interest points by the Harris algorithm [3] and the matching of these points by the correlation measure ZNCC [16, 22], the homography between the two images is estimated from four matches by using RANSAC algorithm [2]. The relationships between the projection matrices, homographies and the images of the absolute conic proved a non-linear cost function. The minimization of this function by the Levenberg-Marquardt [1] allows obtaining the intrinsic parameters of the used camera.

In addition, the importance of this work resides on the one hand in the use of fewer images (two images) instead of using more images [10] to estimate the cameras parameters. On the other hand, it resides in the formulation of self-calibration equations from the matches (numerous and easy to detect) and not of the number of the images (requires a high processing time). The self-calibration steps of our approach are presented in Figure 1.

The paper is organized as follows: Section 2 presents a survey of related works. The camera model used in this work and the image of the absolute conic is treated in Section 3. The vision system is described in Section 4. The tools for self-calibration are presented in Section 5. The self-calibration equations are elaborated in Section 6. Experiments are presented in Section 7, and the conclusions in Section 8.

2. Survey of Related Works

In literature we find several methods which treat the problem of self-calibration. Two categories of these methods can be distinguished: *i)* the methods that use cameras characterized by constant parameters. *ii)* those which use cameras characterized by varying parameters.

i) With the assumption of constant parameters we find several works. The first major work of self-calibration was treated in [4], the authors have proposed an algorithm based on two steps: In the first step, they found the epipolar transformation by the method of Sturm (this method is based on projective invariants) and the other method is based on the generalization of the essential matrix. In the second step of the computation, they used the Kruppa equations [13] which link the epipolar transformation to the image of the absolute conic. Subsequently, in [7] the authors treated the self-calibration of camera
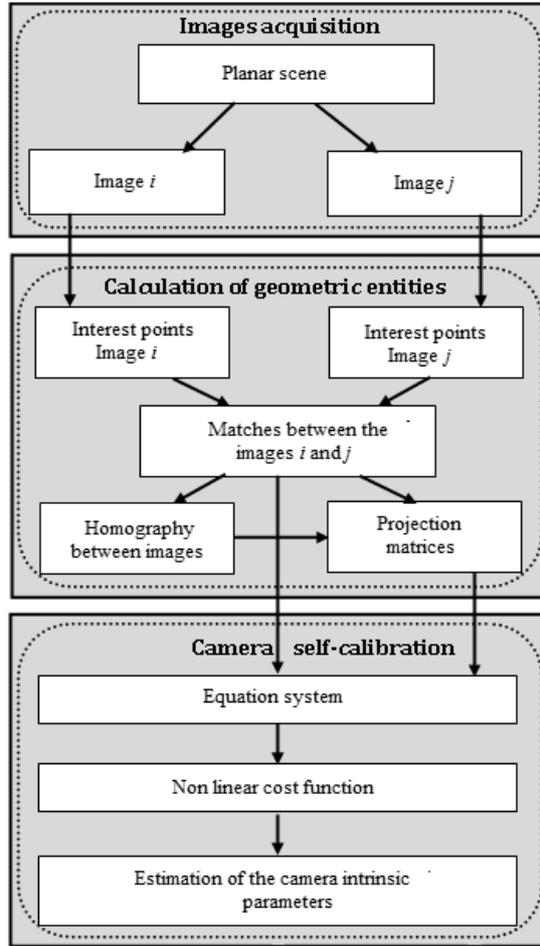
Fig. 1. Steps of camera self-calibration

by using the absolute dual quadric to recover the Euclidean structure. With the same assumption, in [11] the authors have proposed an algorithm based on the projection of two circular points of the planar scene in each image plan (five images at least), together with the estimation of the homography between each couple of images to determine the camera parameters. On the other hand, in [8] the authors have incorporated the so-called module in the stratification approach to upgrade projective structures to affine and finally recover the absolute conic and improve structures Euclidean constraint. Further work

with the same assumption, using 2D or 3D scenes assuming contain specific objects (parallelogram, circle, triangle...) that allow to exploit some geometric constraints to estimate camera parameters. For example, in [26], the authors have proposed a method of self-calibration plane based on the use of a parallelogram. They have used the matched points to estimate all the projection matrices of this parallelogram. These matrices are operated with homographies between images to estimate the intrinsic parameters.

ii) In recent years, the researchers have proposed new methods of camera self-calibration with varying parameters. They have supposed assumptions about the scene (2D or 3D), camera movement (circular, pure rotation), and intrinsic parameters (zero skew and known aspect ratio) for estimating the camera parameters. A new method of self-calibration of camera characterized by the varying intrinsic parameters is treated in [29]. It is based on the quasi-affine reconstruction. After this reconstruction, the authors have estimated the homography of the plane at infinity and they have used it with some constraints on the images of the absolute conic to determine the intrinsic the cameras parameters. On the other hand, a robust method of self-calibration of the cameras characterized by varying parameters is treated in [31]. The last method is based on the projection of three points of the scene on the plans of images and the relation between the matchings to formulate a non-linear cost function. The resolution of the latter allows obtaining the intrinsic parameters of the cameras used. In [23] a method of self-calibration of a camera with varying parameters is based on a circular movement of the camera. The homography of the plane at infinity is determined from two constraints: the first considers that rotation angle between two views of the camera is known, and the second considers that the pixels are square. After obtaining the homography, the intrinsic camera parameters are easily determined. In [17], the authors have considered a self-calibration problem of a moving camera whose intrinsic parameters are known, except the focal length which may vary freely across different views. Furthermore, the focal length's values depend only on the camera's motions. The authors gave a complete catalog of critical motion sequences, which is used to determine these sequences from stereo systems with variable focal. With the assumption of varying parameters, in [27] the authors have presented a practical algorithm for self-calibrating of a camera with varying intrinsic parameters. For each view, the authors suggest minimizing a non-linear least square to establish the matrix of intrinsic parameters. The minimization procedure begins by an initialization to give a first estimate of the focal distance; therefore the estimation of the intrinsic parameters is performed by an algorithm with several iterations. In each iteration, one parameter is estimated by assuming some constraints on the other parameters. A recent method [30] is based on relative distances to estimate the camera parameters. The latter are obtained from the resolution of a non-linear equation system which is formulated by using the invariant relative distance and the homography that transforms the projective reconstruction to metric reconstruction.

The method presented in this work is a development of the work treated in [28] and almost similar to the work treated in [26] and [31]. In [26] and [28], the authors considered that the camera used has constant intrinsic parameters and requires at least three images to calibrate the camera. Moreover, the authors assumed the constraints $\tau = 0$ and $\varepsilon = 0$. On the contrary, the present method uses any camera (characterized by varying intrinsic parameters), in addition, two images are sufficient to calibrate the camera and no constraint on the intrinsic parameters of the camera used. Furthermore, the only difference between this method and the one treated in [31] resides in the objects used in planar scenes: the method presented in [31] is based on the projection of a parallelogram on the plans of images and the relationship between the matches. On the contrary, the present method is based only on the relations between the vertices of the triangles used in the planar scene.

3. Camera Model and the Image of The Absolute Conic

Our approach is based on the pinhole model of the camera to transform a point of the planar scene to its projection in the image.
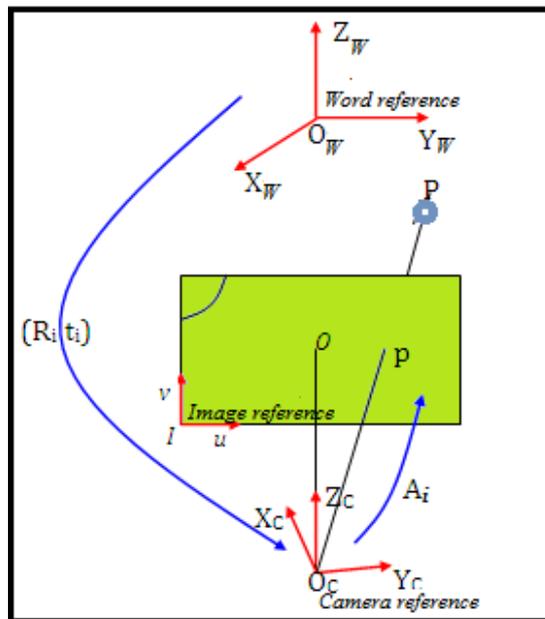
Fig. 2. Pinhole model of camera

The projection of each point P of the scene in image i can be described by a 3×4 matrix: L_i which is expressed by the following formula:

$$p \sim L_i P \tag{1}$$

The matrix L_i can be written as follows: $L_i = A_i(R_i t_i)$; with:
- $(R_i t_i)$ represents the matrix of extrinsic parameters, where R_i the rotation matrix and t_i is the translation vector in the space.
- A_i is the matrix of intrinsic parameters, which is:

$$A_i = \begin{pmatrix} f_i & \tau_i & u_{0i} \\ 0 & \varepsilon_i f_i & v_{0i} \\ 0 & 0 & 1 \end{pmatrix} \tag{2}$$

With, f_i represents the focal length for the view i, $i = 1$ or 2 (in our case), ε_i is the aspect ratio, (u_{oi}, v_{0i}) are the coordinates of the principal point in the image i and τ_i is the image skew.

The Image of the Absolute Conic (IAC), denoted by ω_i, is an imaginary point conic directly related to the camera internal matrix A_i in formula (2) via $\omega_i = \left(A_i A_i^T\right)^{-1}$:

$$\omega_i = \frac{1}{\varepsilon_i^2 f_i^4} \begin{pmatrix} \varepsilon_i^2 f_i^2 & -\tau_i \varepsilon_i f_i & -u_{0i} \varepsilon_i^2 f_i^2 + v_{0i} \tau_i \varepsilon_i f_i \\ * & f_i^2 + \tau_i^2 & -v_{0i} f_i^2 + u_{0i} \tau_i \varepsilon_i f_i - v_{0i} \tau_i^2 \\ * & * & \varepsilon_i^2 f_i^4 + v_{0i}^2 f_i^2 + (u_{0i} \varepsilon_i f_i - \tau_i v_{0i})^2 \end{pmatrix} \tag{3}$$

Where the three lower triangular elements are replaced by "$*$" to save space, since ω_i is symmetric. The estimation of intrinsic parameters of the camera used automatically gives the elements of the matrix ω_i and vice versa.

4. Vision System

In this work, we consider an unknown planar scene. On the plan of the scene, we consider n points P_r, with $r = 1 \ldots n$, or $n \in N^*$ and O is a point different from the points P_r and it is in the same plane which contains the points P_r. For each segment $[OP_r]$, there exists a unique point M_r in the scene plan such that $OP_r M_r$ is an equilateral triangle having an angle $P_r \widehat{O} M_r > 0.$. We associate to each triangle $OP_r M_r$ a reference (O, X_r, Y_r, Z_r) with $P_r \in (OX_r)$ and (OZ_r) is perpendicular to the plan containing the triangle $(OP_r M_r)$ (Figure 3).

We denote by (O, X_1, Y_1) the fixed reference in the scene plan. Let (O, X_r, Y_r) with $r = 2 \ldots n$ denote moving references according to (O, X_1, Y_1). These references are associated with equilateral triangles $OP_r M_r$ with $r = 2 \ldots n$. They are obtained by a simple rotation of the fixed reference around (OZ_1) axis. In addition to that, the passage
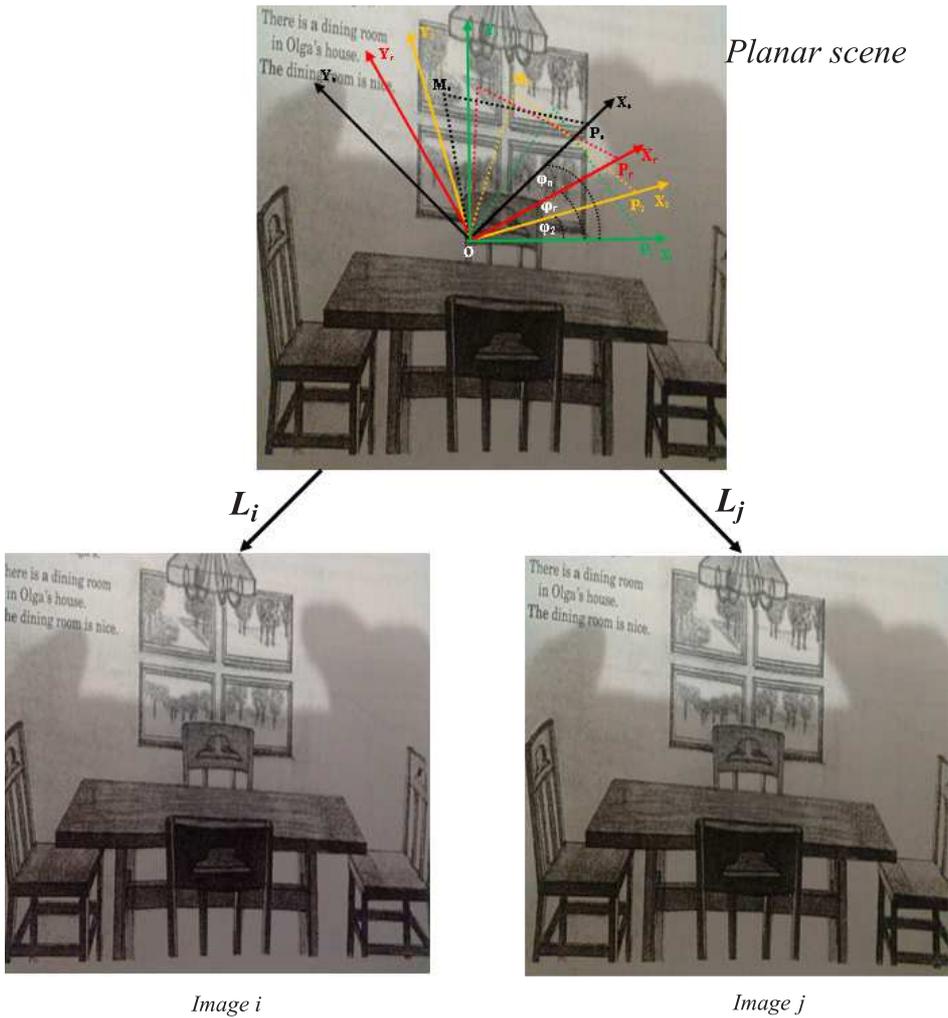
Fig. 3. Vision system

from fixed reference (O, X_1, Y_1) to the moving reference (O, X_r, Y_r) is performed by using the rotation matrix which is given as follows:

$$\Re(\varphi_r) = \begin{pmatrix} \cos(\varphi_r) & -\sin(\varphi_r) & 0 \\ \sin(\varphi_r) & \cos(\varphi_r) & 0 \\ 0 & 0 & 1 \end{pmatrix}, \quad \text{with } r = 2 \ldots n \tag{4}$$

With φ_r the rotation angle which allows obtaining the moving reference (Figure 4).

Figure 4 shows the system used: the planar scene, the fixed reference, the moving references and the equilateral triangles.
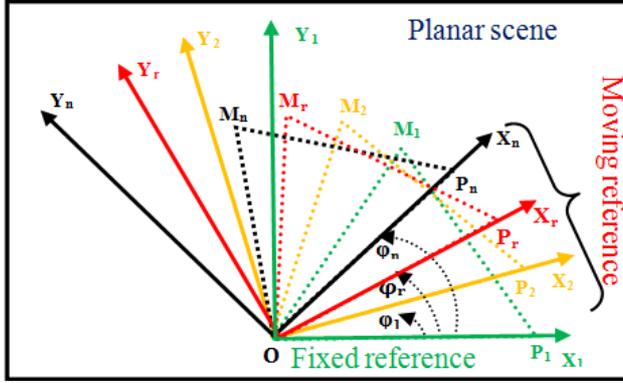
Fig. 4. System used

The homogeneous coordinates of points P_r, M_r and O in the moving reference (O, X_r, Y_r) are respectively $(a_r, 0, 1)^T$, $(\frac{a_r}{2}, \frac{\sqrt{3}}{2}a_r, 1)^T$ and $(0, 0, 1)^T$. With a_r $(a_r = OP_r)$ represents the length of the equilateral triangle OP_rM_r. These coordinates can be rewritten as follows:

$$(a_r, 0, 1)^T = S_r(1, 0, 1)^T \tag{5}$$

$$(\frac{a_r}{2}, \frac{\sqrt{3}}{2}a_r, 1)^T = S_r(0, 1, 1)^T \tag{6}$$

With:

$$S_r = \begin{pmatrix} a_r & \dfrac{a_r}{2} & 0 \\ 0 & \dfrac{\sqrt{3}}{2}a_r & 0 \\ 0 & 0 & 1 \end{pmatrix} \tag{7}$$

The coordinates corresponding to points P_r and M_r in the fixed reference can be calculated as follows: $\mathfrak{R}(\varphi_r)P_r$ and $\mathfrak{R}(\varphi_r)M_r$.

5. Self-calibration Tools

The self-calibration procedure used in our approach is the following: detecting the interest points by Harris algorithm, setting a matching of the interest points by the correlation measure ZNCC, calculating the homography between images using the RANSAC

algorithm, determining the projection matrix of the scene by the resolution of a linear system, and estimating the intrinsic parameters of the camera used by minimizing of a non-linear cost function.

5.1. Matching and interest points

The matching of the image points can be established in two steps: The first step is to extract the interest points of the two images i and j. In the literature, there are several algorithms to extract interest points [3, 9, 20, 21], this article uses the Harris algorithm [3].The second step is to find for each interest point of the image their correspondent in the image by measuring correlation ZNCC [16, 22], and then we eliminate the false matches by using the RANSAC algorithm [2].

5.2. Homography between images

The homography is a $3{\times}3$ transformation of matrix linking the matches points between the images i and j, it is expressed as follows:

$$p_{jr} \sim H_{ij}p_{ir} \tag{8}$$

Where p_{ir} and p_{jr} are respectively the projection of a point P_r of the scene in the images i and j. With $r = 1 \ldots n$, H_{ij} is the homography matrix between the images i and j. The homography matrix is calculated by the RANSAC algorithm [2]. The latter allows estimating the geometric entity (homography) from four matches between the images i and j.

5.3. Projection matrices of the segments $[OP_r]$

The objective of this section is to estimate the projection matrices L_{ir} and L_{jr} for each segment $[OP_r]$ of the scene, in the two images i and j (Figure 5). Knowing that the degree of freedom of these matrices is eight, therefore, we need at least eight equations to calculate these two matrices which will be used in the self-calibration equations.

The projection of the different points expressed in the fixed reference of the scene in the images i and j is given by the formula (1). The coordinates of the points P_r in the fixed reference are given by $\Re(\varphi_r)P_r$, and they are given by $S_r(1,0,1)^T$ in the moving reference (O, X_r, Y_r).

The projection of the points $O, P_1, P_2, \ldots, P_n$ in the images i and j is performed by the following formulas:

$$Image\ i \Rightarrow \begin{cases} (u_{i0}, v_{i0}, 1)^T & \sim & L_{ir}(0,0,1)^T \\ (u_{ip_r}, v_{ip_r}, 1)^T & \sim & L_{ir}(1,0,1)^T \end{cases} \tag{9}$$

$$Image\ j \Rightarrow \begin{cases} (u_{j0}, v_{j0}, 1)^T & \sim & L_{jr}(0,0,1)^T \\ (u_{jp_r}, v_{jp_r}, 1)^T & \sim & L_{jr}(1,0,1)^T \end{cases} \tag{10}$$
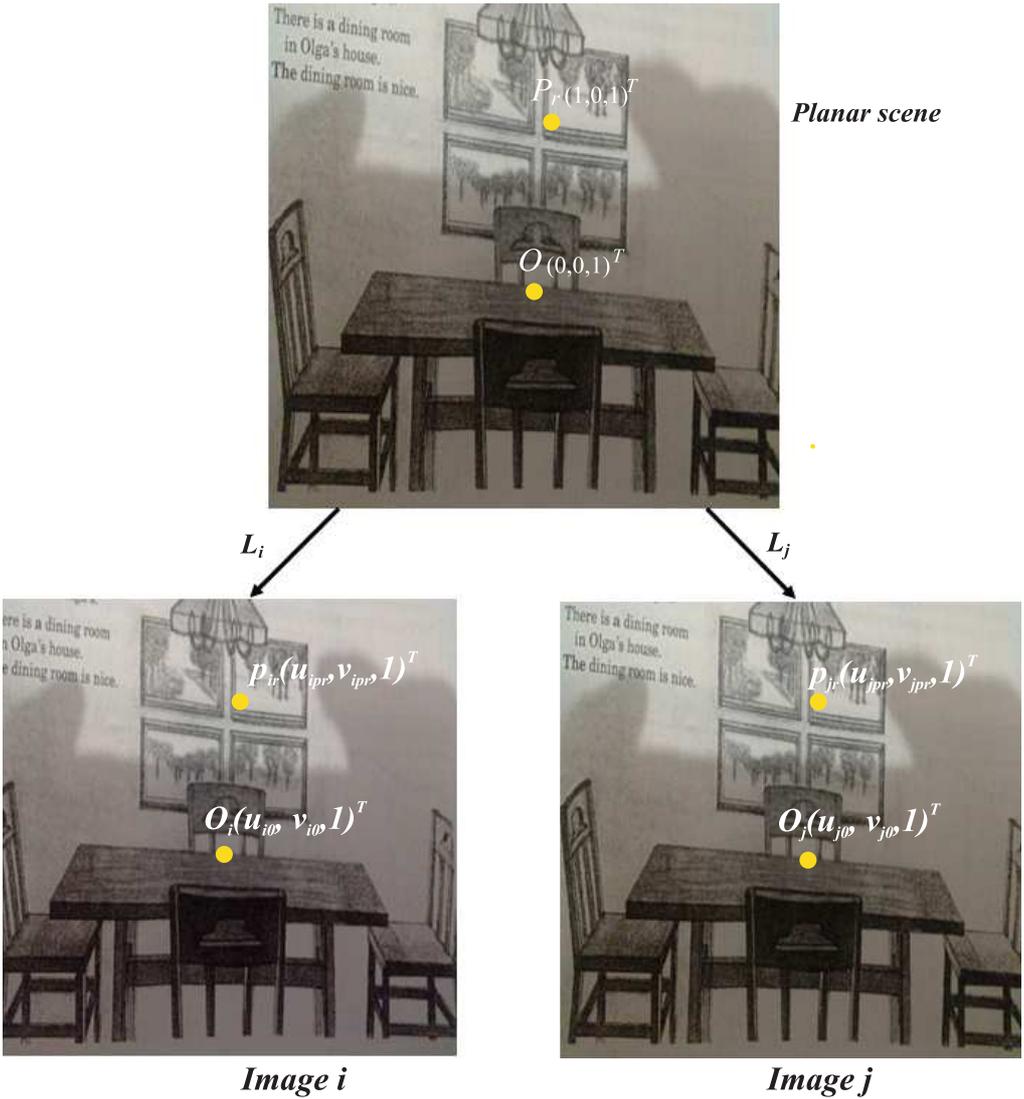
Fig. 5. Projection of points of the scene in the images i and j

With the points $(u_{i0}, v_{i0}, 1)^T$ and $(u_{ip_r}, v_{ip_r}, 1)^T$ are respectively the projection of the points O and P_r in the image i, the points $(u_{j0}, v_{j0}, 1)^T$ and $(u_{jp_r}, v_{jp_r}, 1)^T$ are respectively the projection of the points O and P_r in the image j and L_{ir}, L_{ir} represent the

projection matrices of the points (O, P_r) in the images i and j respectively, they are expressed as follows:

$$L_{ir} = A_i R_i \begin{pmatrix} 1 & 0 & \\ 0 & 1 & R_i^T t_i \\ 0 & 0 & \end{pmatrix} \mathfrak{R}(\varphi_r) S_r \tag{11}$$

$$L_{jr} = A_j R_j \begin{pmatrix} 1 & 0 & \\ 0 & 1 & R_j^T t_j \\ 0 & 0 & \end{pmatrix} \mathfrak{R}(\varphi_r) S_r \tag{12}$$

With $\mathfrak{R}(\varphi_r)$ and S_r are given respectively by the formulas (4) and (7).

Let S^* denotes the matrix is defined as follows: $S_r^* = \mathfrak{R}(\varphi_r) S_r$. Using the formulas (4) and (7), S_r^* can be expressed as follows:

$$S_r^* = \begin{pmatrix} a_r \cos(\varphi_r) & \dfrac{a_r}{2} \cos(\varphi_r) - \dfrac{\sqrt{3}}{2} a_r \sin(\varphi_r) & 0 \\ a_r \sin(\varphi_r) & \dfrac{a_r}{2} \sin(\varphi_r) + \dfrac{\sqrt{3}}{2} a_r \cos(\varphi_r) & 0 \\ 0 & 0 & 1 \end{pmatrix} \tag{13}$$

The matrices $H_i = A_i R_i \begin{pmatrix} 1 & 0 & \\ 0 & 1 & R_i^T t_i \\ 0 & 0 & \end{pmatrix}$ and $H_j = A_j R_j \begin{pmatrix} 1 & 0 & \\ 0 & 1 & R_j^T t_j \\ 0 & 0 & \end{pmatrix}$ are respectively the homographies which permit to project the plane of the scene, in the images i and j, therefore the formulas (11) and (12) become:

$$L_{ir} = H_i S_r^* \tag{14}$$

$$L_{jr} = H_j S_r^* \tag{15}$$

From Equations (14) and (15) we deduce that:

$$L_{jr} = H_{ij} L_{ir} \tag{16}$$

With H_{ij} is the homography between the images i and j such that:

$$H_{ij} = H_j H_i^{-1} \tag{17}$$

From the formulas (11), (12) and (13) we can deduce that:

$$L_{ir} = A_i R_i (G_r R_i^T t_i) \tag{18}$$

$$L_{jr} = A_j R_j (G_r R_j^T t_j) \tag{19}$$

With:

$$G_r = \begin{pmatrix} a_r \cos(\varphi_r) & \dfrac{a_r}{2}\cos(\varphi_r) - \dfrac{\sqrt{3}}{2}a_r\sin(\varphi_r) \\ a_r \sin(\varphi_r) & \dfrac{a_r}{2}\sin(\varphi_r) + \dfrac{\sqrt{3}}{2}a_r\cos(\varphi_r) \\ 0 & 0 \end{pmatrix} \tag{20}$$

The formula (9) gives four equations according to the L_{ir} elements.
The formulas (10) and (16) give:

$$\begin{cases} (u_{j0}, v_{j0}, 1)^T \sim H_{ij} L_{ir}(0,0,1)^T \\ (u_{jp_r}, v_{jp_r}, 1)^T \sim H_{ij} L_{ir}(1,0,1)^T \end{cases} \tag{21}$$

The system (21) gives four other equations according to the L_{ir} elements;
Therefore, we can obtain the eight L_{ir} elements from expressions (9) and (21).
The L_{jr} projection matrix is estimated from the formula (16).

6. Camera Self-Calibration

The expression (18) gives:
$$A_i^{-1} L_{ir} = R_i(G_r R_i^T t_i) \tag{22}$$

The formula (22) can be written as follows:

$$L_{ir}^T \omega_i L_{ir} = \begin{pmatrix} G_r^T G_r & G_r R_i^T t_i \\ t_i^T R_i G_r & t_i^T t_i \end{pmatrix} \tag{23}$$

With $\omega_i = (A_i A_i^T)^{-1}$ is the projection of the absolute conic ($\Omega \sim I_3$) in the image i.
Proceeding in the same way, we can show that:

$$L_{jr}^T \omega_j L_{jr} = \begin{pmatrix} G_r^T G_r & G_r R_j^T t_j \\ t_j^T R_j G_r & t_j^T t_j \end{pmatrix} \tag{24}$$

With $\omega_j = (A_j A_j^T)^{-1}$ is the projection of the absolute conic ($\Omega \sim I_3$) in the image j.
The expression (20) gives:

$$G_r^T G_r = \begin{pmatrix} a_r^2 & \dfrac{a_r^2}{2} \\ \dfrac{a_r^2}{2} & a_r^2 \end{pmatrix} \tag{25}$$

From the formulas (23) and (24) we can deduce that the four upper left coefficients $(G_r^T G_r)$ of $L_{ir}^T \omega_i L_{ir}$ and $L_{jr}^T \omega_j L_{jr}$ are identical.

We note by Q_{ir} and Q_{jr} the matrices that represent respectively the four upper left coefficients $(G_r^T G_r)$ of the two matrices $L_{ir}^T \omega_i L_{ir}$ and $L_{jr}^T \omega_j L_{ijr}$.

From expressions (23) and (24), we conclude that:

$$Q_{ir} \sim Q_{jr} \tag{26}$$

We put:

$$Q_{ir} = \begin{pmatrix} q_{1ir} & q_{2ir} \\ q_{2ir} & q_{1ir} \end{pmatrix} \tag{27}$$

and

$$Q_{jr} = \begin{pmatrix} q_{1jr} & q_{2jr} \\ q_{2jr} & q_{1jr} \end{pmatrix} \tag{28}$$

From the equations (26), (27) and (28) we can deduce the following equalities between images i and j:

$$\frac{q_{1ir}}{q_{2ir}} = \frac{q_{1jr}}{q_{2jr}} \quad \text{with} \quad r = 1 \ldots n \tag{29}$$

Where n represents the number of matches between images i and j.

The expression (29) gives:

$$q_{1ir} q_{2jr} - q_{1jr} q_{2ir} = 0 \quad \text{with } r = 1 \ldots n \tag{30}$$

Therefore, for each couple (p_{ir}, p_{jr}), we obtain one equations. Then we need at least ten matching couples to estimate the ten parameters of the camera used. Indeed, with this approach we detect an important number of matched points couples (n matches) which provides a large number of equations (n equations). Furthermore, the importance of this approach lies in the fact that the self-calibration equations become related to the couples of the matched points.

The system (30) is non-linear; therefore, we will minimize the following non-linear cost function:

$$\min_{(\omega_i, \omega_j)} \sum_{i=1}^{m-1} \sum_{j=i+1}^{m} \sum_{r=1}^{n} \left(q_{1ir} q_{2jr} - q_{1jr} q_{2ir} \right)^2 \tag{31}$$

With m represents the number of images, and n represents the number of matches.

To solve the function (31) we use the Levenberg-Marquardt algorithm [1]. The latter requires an initialization step. For this, we assume that some conditions are satisfied on the vision system.

- The pixels are squared therefore $\varepsilon_i = \varepsilon_j = 1$ and $\tau_i = \tau_j = 0$.
- The principal point is in the center of the images, therefore: $u_{0i} = v_{0i} = u_{0j} = v_{0j} = 256$ (because the size of images used is 512×512). And the focal lengths (f_i, f_i) are estimated from the expression (30) (by replacing the parameters by their values in this expression).

7. Experimentation

7.1. Simulations

In this section, we realize a simulation of a sequence of ten 512×512 images of an unknown planar scene to show the performance and robustness of our approach. We estimated the camera parameters by a classical method of calibration from a planar pattern, the parameters obtained are as follows: $f = 1230$, $\varepsilon = 0.93$, $u_0 = 261$ and $v_0 = 254$. In the
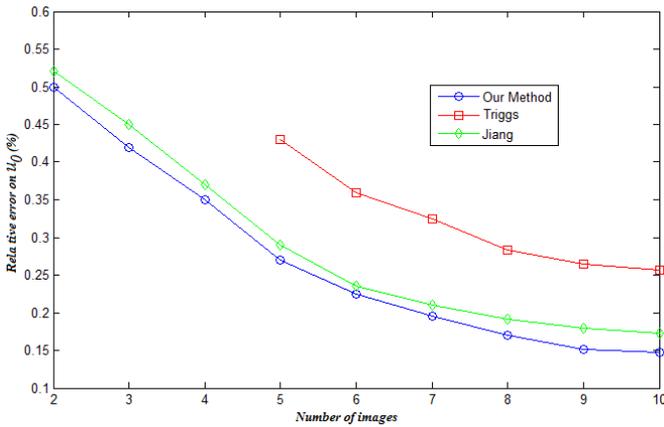
Fig. 6. Relative error on u_0 (%) according to number of images
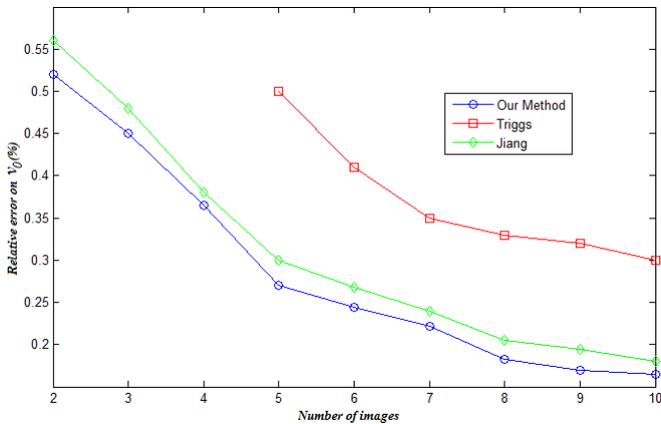
Fig. 7. Relative error on v_0 (%) according to number of images
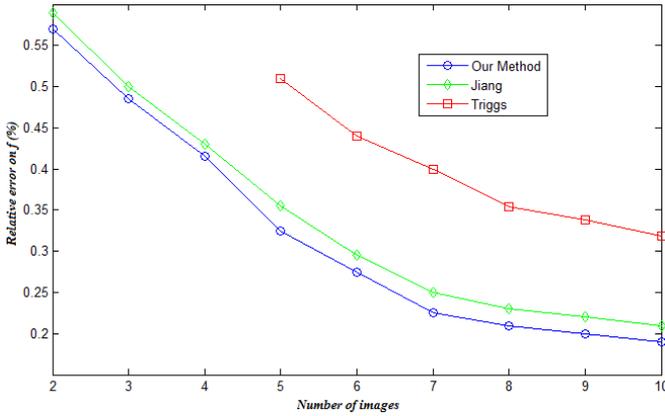
Fig. 8. Relative error on f (%) according to number of images
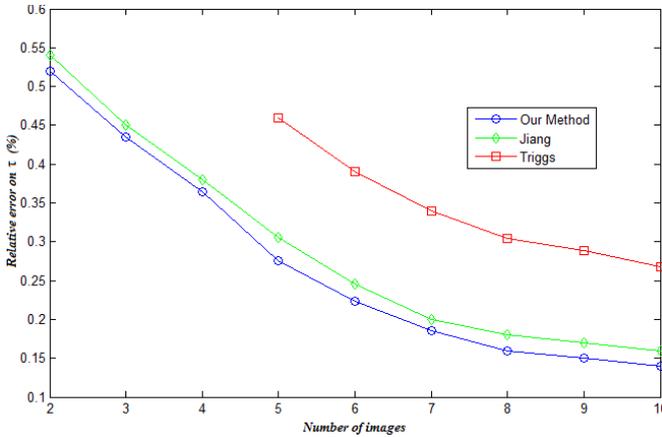
Fig. 9. Relative error on τ (%) according to number of images

first time, we have carried the detection of interest points by Harris algorithm [3], and we have matched these points by the ZNCC correlation function [16, 22] aiming to estimate the homographies (from the 4 matches) between couples of images by the RANSAC algorithm [2]. These homographies are used with the projection of the planar scene points in the images to determine the different projection matrices. The resolution of a non-linear equation system which is formulated from the points of the planar scene and its projections in the images (the matches) by Levenberg-Marquardt algorithm [1] allows
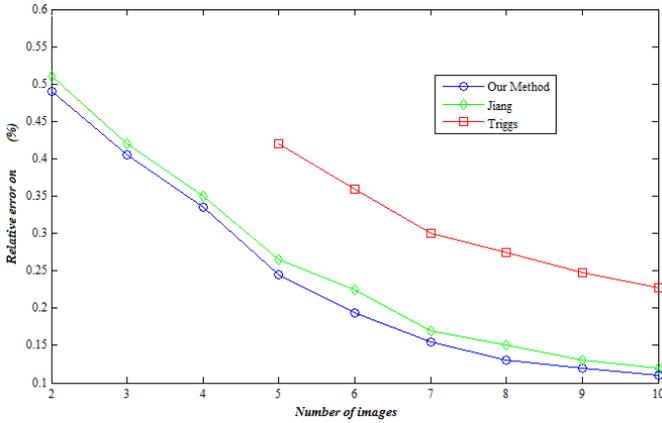
Fig. 10. Relative error on ε (%) according to number of images
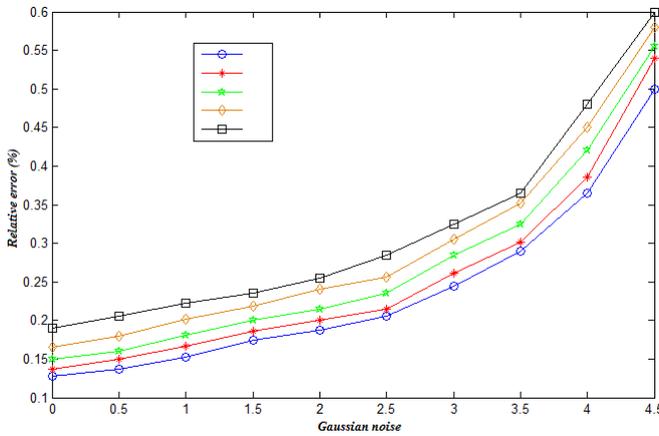
Fig. 11. Relative error on $(u_0, v_0, \varepsilon, \tau)$ and f (%) according to Gaussian noise

to treat the intrinsic parameters of the different cameras used. For this, we compare our method with two other efficient methods which are Triggs [11] and Jiang [29]. In this simulation, we discussed the influence of the number of images used on the relative errors corresponding to u_0, v_0, ε, τ and f (represented respectively in Figures 6, 7, 8, 9 and 10) by our approach and the approaches of Triggs [11] and Jiang [29].

We also carry out a second simulation to test the performance of our method with respect to noise. To do this, we add to all image pixels a Gaussian white noise with

standard deviation σ $(0 < \sigma \leq 4.5)$ with a step of 0.5. For each noise level, we calculate the relative errors corresponding to u_0, v_0, ε and f (represented in Figure 11) by our approach.

7.2. Analysis of the simulations

The Figures 6, 7, 8, 9 and 10 show that relative errors corresponding to u_0, v_0, ε, τ and f determined by our method decrease almost linearly if the number of images is between 2 and 5. They decrease slowly when the number of images used is between 5 and 8. They become almost stable if the number of images exceeds 8, but when the number of images increases, the parameters to be estimated become very numerous. Consequently, the calculations become more complex, which allows increasing the program execution time.

On the other hand, the Figure 11 shows that the relative errors to u_0, v_0, ε, τ and f remain almost stable when the noise value is between 0 and 2.5. They increase slowly if the noise is between 2.5 and 3.5, and they increase quickly if the noise becomes greater than 3.5.

The analysis of the results obtained in Figures 6, 7, 8, 9 and 10, shows that the relative errors corresponding to the parameters u_0, v_0, ε, τ and f obtained by our method are similar to those calculated by the method of Jiang [29], and they are a little different to those obtained by the method of Triggs [11]. Triggs uses more than four images to estimate the intrinsic parameters. On the contrary, our method estimates the parameters of the camera used from two images only.

7.3. Real data

Ten 512×512 images of an unknown planar scene are taken by a digital camera characterized by varying parameters from different views to confirm the robustness of the approach presented in this paper. Two (among ten) are shown in Figure 12(a). The interest points and the matches between these two images are shown respectively in Figure 12(b) and Figure 12(c).

For the choice of equilateral triangles in the images shown in Figure 12(c), we denote by (o_i, o_j) a matching between the images i and j, such that (o_i, o_j) are the projections of the origin of the fixed reference in the images i and j. Moreover, let (p_{ri}, p_{rj}) a couple of matching between the images i and j such that p_{ri} and p_{rj} are the projections of the second vertex of the triangle respectively in the images i and j. There exists a unique point M_r in the scene plan such that $OP_r M_r$ is an equilateral triangle, the point M_r is not used in practice (we only projected two points o and P_r in the images, because their correspondents in these images represent a couple of matching).

In our approach, the estimation of the intrinsic parameters is based on the couples of matched points. To obtain efficient solutions, we have performed a regularization phase.

(a)

(b)

(c)
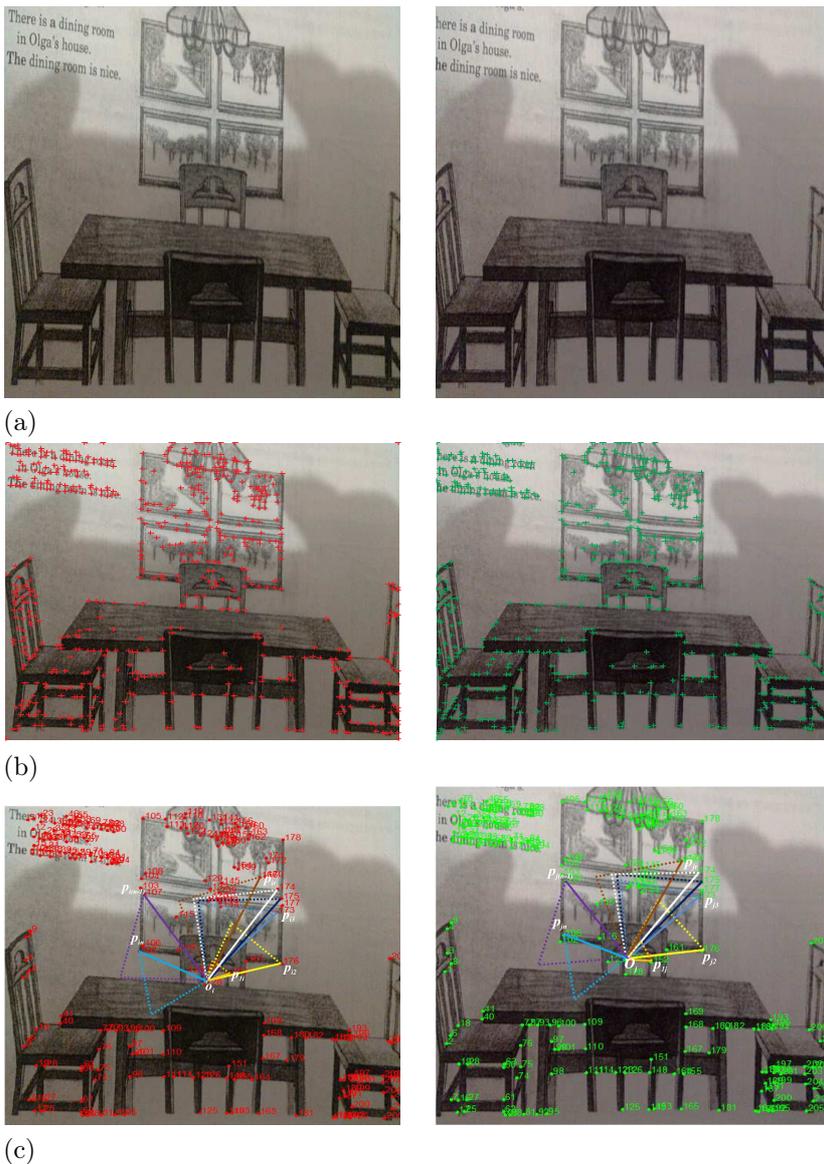
Fig. 12. (a) The two images of the planar scene. (b) The interest points detected by Harris. (c)
The matches between the couple of images.

Indeed, the couples of matched points in this phase contain false matches; we eliminate them by the constraint that checks the formula (8).

The projection of the points of the planar scene in the two images allows estimating the geometric entities (the homographies and the projection matrices). Afterwards, the solution of a non-linear system of equations (formula (31)) allows estimating the elements the image of the absolute conic and finally the intrinsic parameters of the camera.

The Table 1 below represents the intrinsic parameters estimated by our approach.

Tab. 1. The Results of Intrinsic Camera Parameters Estimated by the Two Methods

		f	ε	τ	u_0	v_0
The present method	Image 1	1237	0.93	0.04	258	262
	Image 2	1233	095	0.03	260	254
	Image 3	1247	0.92	0.01	253	259
	Image 4	1251	0.94	0.02	257	261
Jiang	Image 1	1249	1	0	251	259
	Image 2	1243	0.93	0.05	263	261
	Image 3	1255	0.95	0.02	259	264
	Image 4	1267	0.91	0.04	251	260

According to the experiments results on real data: the two images presented in Figure 12(a) and the eight other images, we conclude that our approach gives the results closer to those obtained by Jiang [29].This shows, on the one hand, the accuracy of the approach presented in this present work. In the other hand, our algorithms converge rapidly to the optimal solution, because we estimated the five parameters of the camera for each view, knowing that we did not use any constraint on the intrinsic parameters of the camera, on the contrary, Jiang assumes that $\tau = 0$ and $\varepsilon = 1$ in the first image. These constraints influence directly the results of self-calibration. Our method and Jiang's can calibrate the camera from only two images, but the suggested method presents the advantage does not require any constraint on the self-calibration system, compared to Jiang method which requires the constraints on intrinsic parameters of the camera.

8. Conclusion

In this work, the problem of the self-calibration of cameras with varying intrinsic parameters has been addressed by using an unknown planar scene. This approach is based on the use of equilateral triangles assumed in the planar scene and the transformation matrix between them. The projection of vertices of equilateral triangles in the planes of the images and , and the relationship between images of absolute conic for each pair of

images allow formulating a non-linear cost function. The minimization of this function by the Levenberg-Marquardt algorithm provides the intrinsic parameters of the cameras used. The advantages of this method are the use of any camera (no constraints on the intrinsic parameters) and two images of the planar scene are sufficient to calibrate the cameras used. The found experiments results are satisfactory, which shows the robustness and reliability of our approach.

References

1977

[1] J. More : The Levenberg-Marquardt Algorithm, Implementation and Theory. In G. A. Watson, editor, Numerical Analysis, Lecture Notes in Mathematics 630. Springer-Verlag, pp. 105-116.

1981

[2] M. A. Fischler and R. C. Bolles : Random sample consensus: A Paradigm for Model Fitting with Applications to Image Analysis and Automated Cartography. Graphics and Image Processing, pp. 381-395.

1988

[3] C. Harris and M. Stephens : A combined Corner et Edge Detector. 4th Alvey vision Conference. pp. 147-151.

1992

[4] O. Faugeras, Q.-T. Luong, S. Maybank : Camera Self-Calibration: Theory and Experiments . In: G. Sandini (Ed.), Proceedings of the European Conference on Computer Vision, Springer-Verlag, pp. 321-334.

[5] S. J. Maybank and O. D. Faugeras : A Theory of Self Calibration of a Moving Camera. International Journal on Computer Vision, pp. 123-151.

1994

[6] R. I. Hartley : Self-Calibration From Multiple Views with a Rotating Camera. In ECCV, pp. 471-478.

1996

[7] A. Heyden, K. Aström : Euclidean Reconstruction from Constant Intrinsic Parameters. In: Proc. International Conference on Pattern Recognition, pp. 339-343.

[8] M. Pollefeys, L.V. Gool, M. Oosterlinck : The Modulus Constraint: A New Constraint for Self-Calibration. In: Proc. Int. Conf. on Pattern Recognition, pp. 349-353.

1997

[9] S. M. Smith and J. M. Brady : SUSAN - A New Approach to Low Level Image Processing. International Journal of Computer Vision, 45-78.

1998

[10] M. Pollefeys, R. Koch and L. Van Gool : Self-Calibration and Metric Reconstruction in Spite of Varying and Unknown Internal Camera Parameters. ICCV, pp. 90-95.

[11] B. Triggs : Autocalibration from Planar Sequences. In Proceedings of 5th European Conference on Computer Vision, pp. 89-105.

1999

[12] P. F. Sturm and S. J. Maybank : On Plane-Based Camera Calibration: A General Algorithm, Singularities, Applications. In Proceedings of the CVPR-IEEE, pp. 432-437.

2000

[13] P. Sturm : A Case Against Kruppa's Equations for Camera Self-Calibration. IEEE Transactions on Pattern Analysis and Machine Intelligence, pp. 1199-1204.

[14] Z. Zhang : A Flexible New Technique for camera Calibration. IEEE Transactions on Pattern Analysis and Machine Intelligence. pp. 1330-1334.

2001

[15] M. Wilczkowiak, E. Boyer, P. Sturm : Camera Calibration and 3D Reconstruction from Single Images Using Parallelepipeds. In ICCV, Vancouver, pp. 142-148.

2002

[16] M. Lhuillier and L. Quan : Quasi-Dense Reconstruction from Image Sequence. ECCV.

[17] P. Sturm : Critical motion sequences for the self-calibration of cameras and stereo systems with variable focal length. Image and Vision Computing, 20(5-6): 415-426.

2003

[18] P. Gurdjos and P. Sturm : Methods and Geometry for Plane-Based Self-Calibration. CVPR, pp. 491-496.

[19] P. Liu, J.Shi, J. Zhou and L. Jiang : Camera Self-Calibration Using the Geometric Structure in Real Scenes. In: Proceedings of the Computer Graphics International, pp. 262-265.

2004

[20] D. G. Lowe : Distinctive Image Features from Scale-Invariant Keypoints. International Journal of Computer Vision, 91-110.

2006

[21] B. Bouda, Lh. Masmoudi and D. Aboutajdine. A New Grey Level Corner Detection Based on Electrostatic Model. ICGST-GVIP, 21-26.

[22] A. Saaidi, H. Tairi and K. Satori : Fast Stereo Matching Using Rectification and Correlation Techniques. ISCCSP, 2nd International Symposium on Communications, Control and Signal Processing.

2008

[23] Y. Li, Y.S. Hung, S. Lee : A Stratified Self-Calibration Method for Circular Motion in Spite of Varying Intrinsic Parameters. Image and Vision Computing, pp. 731-739.

[24] A. Saaidi, A. Halli, H. Tairi and K. Satori : Self -Calibration Using a Particular Motion of Camera. In WSEAS Transaction on Computer Research, pp. 295-299.

2009

[25] J. Kima, I. Kweon : Camera calibration based on arbitrary parallelograms. Computer Vision and Image Understanding, pp. 1-10

[26] A. Saaidi, A. Halli, H. Tairi and K. Satori : Self-Calibration Using a Planar Scene and Parallelogram. ICGST-GVIP, pp. 41-47.

2011

[27] A. El-attar, M. Karim, H. Tairi, S. Ionita : A Robust Multistage Algorithm for Camera Self-Calibration Dealing with Varying Intrinsic Parameters. JATIT, pp. 46-54.

2012

[28] A. Baataoui, I. El Batteoui, A. Saaidi and K. Satori : Camera Self-Calibration by an Equilateral Triangle. International Journal of Computer Applications, pp. 29-34.

[29] Z. Jiang, S. Liu : Self-calibration of Varying Internal Camera Parameters Algorithm Based on Quasi-affine Reconstruction. Journals of Computers, pp. 774-778.

[30] Y. Shang, Z. Yue, M. Chen and Q. Song : A New Method of Camera Self-Calibration Based on Relative Lengths. Information Technology Journal, pp. 376-379.

2013

[31] N. El Akkad, M. Merras, A. Saaidi, and K. Satori : Robust Method for Self-Calibration of Cameras Having the Varying Intrinsic Parameters. JATIT, pp. 57-67.